Using Artificial Intelligence Techniques For Reconstructing GRACE Data Over Nile River

Basma Fawzi[1*], Mahmoud Salah[2], and Mahmoud El-Mewafi[3]

[1] Department of Civil Engineering, Delta Higher Institute for Engineering and Technology, Mansoura 35111, Egypt
[2] Department of Geomatics, Faculty of Engineering Shoubra, Benha University 13518, Egypt
[3] Public Works Department, Faculty of Engineering, Mansoura University 35111, Egypt
[*] Corresponding author. E-mail: basma.fawzi283@gmail.com

Received: July 03, 2024; Accepted: September 19, 2024

Terrestrial water storage (TWS) is crucial for the worldwide hydrologic water cycle and sustainability of water. Gravimetric missions such as the Gravity Recovery and Climate Experiments (GRACE) & GRACE-Follow on (GRACE-FO) are essential for evaluating changes in TWS.This study introduces a new approach by combining remote sensing data in the form of mascon data with deep learning models (DL) such as the Long Short-Term Memory (LSTM) Model to reconstruct GRACE data in the Nile River basin (NRB) from 2002 to 2022 to study the changes in water storage with high accuracy. This research strategy depends on applying several convolutional neural network (CNN) models, including AlexNet, VGG Net, and GoogleNet, for extracting features from time series GRACE data. After that, use the optimization algorithm (DTOFGW) to get the best hyperparameters for LSTM. Finally, comparing many different optimization algorithms showed the proposed model's superiority. Applying statistical analysis tests illustrated the significance of our proposed model, such as ANOVA and T-test. The results of the trial showed that the proposed model (DTOFGW-LSTM) outperformed the other models by an accuracy of 96.8%, sensitivity of 0.5, specificity of 99.5%, P value of 0.85, N value of 0.97, F-score of 0.63, and confidence value of 97%.

Keywords: GRACE; GRACE-FO; Artificial Intelligence; LSTM-DTOFGW; ANOVA; T-test

http://dx.doi.org/10.6180/jase.202508_28(8).0001

1. Introduction

The Nile River, which flows through Africa, holds the distinction of being both the longest river on the continent and the longest river globally. The Nile spans approximately 6,650 kilometers (4,130 miles) in length and spans the drainage basin of eleven nations, namely the Democratic Republic of the Congo, Tanzania, Burundi, Rwanda, Uganda, Kenya, Ethiopia, Eritrea, South Sudan, Republic of the Sudan, and Egypt. Particularly, the Nile serves as the predominant water source for Egypt, Sudan, and South Sudan. Moreover, the Nile has a crucial role in enhancing agriculture and fishing industries, therefore contributing significantly to the economy [1].

(TWS) is an essential element of the worldwide hydrological water cycle [2]. Total Water Storage (TWS) encompasses the complete volume of water present on and below the Earth's surface, encompassing moisture in the soil, groundwater, and surface-level water such as lakes, dams, rivers, and glacier water equivalent [3]. (TWS) are mainly affected by land surface water cycle such as: evaporation, temperature, runoff, snow melt and precipitation [4].

GRACE considers the first satellite to be used for estimating Terrestrial Water Storage Changes(TWSC) and it is the only one that can capture data underground surface by measuring the gravity of the Earth with high accuracy [5, 6]. The GRACE-Follow On (GRACE-FO) satellite mission was launched in 2018 by the German Aerospace Center (DLR:

Deutsches Zentrum für Luft), while the Gravity Recovery and Climate Experiment (GRACE) was launched in 2002 by the United States National Aeronautics and Space Administration (NASA) [7]. GRACE data is used to remotely measure changes in regional and global Terrestrial Water Storage Changes (TWSC) for major river basins (>200,000 km^2) with monthly temporal resolution [8].

More investigation for TWSC in Nile basin were made to study the change in water storage depending on GRACE data from multi solution centers and the results indicated that the mascon's data outperformed GRACE spherical harmonic solutions in terms of uncertainty. The evapotranspiration correlation (R^2 = 0.85), followed by the normalized differential vegetation index (R^2 = 0.82), Reducing groundwater and soil moisture from 2003 to 2017 indicate that drought may be a probable in Nile basin [9].

Deep learning models like a novel restoration approach for compressed sensing (CS) that combines convolutional neural networks (CNNs) and the Bayesian inference method is called Bayesian Convolutional Neural Networks (BCNNs). Bayesian convolutional neural networks (BCNN) have recently been used to predict (TWSC)by automatically generating crucial (TWSC)prediction features from multisource input data. (TWSC) predictions are compared to hydrological model output and three current (TWSC) prediction products. BCNN predicts gap (TWSC) better, especially in arid regions. BCNN's ability to detect extreme dry and wet events throughout the interglacial period is demonstrated by comparing precipitation changes, drought index, ground/surface water levels, and other variables. BCNN can maintain (TWSC) data continuity and identify climate anomalies during the data gap [10].

This research aims to reconstruct TWSC for the Nile River basin using GRACE mascon data and artificial intelligence models. The proposed model was used to improve the reconstruction and validation data accuracy. In the following sections, section 2 explains the methodologies employed and the data sets utilized in NRB. Section 3 describes the results of the suggested model applied to the NRB in detail. Discussion of the GRACE data of Terrestrial Water Storage Changes (TWSC)reconstruction work is presented in Section 4. Finally, section 5 presents a summary of the results of this study.

2. Materials and methods

2.1. Study Area

This study focuses on the Nile River basin (NRB), which spans approximately 35 degrees of latitude from South to North, as depicted in Fig. 1. The Nile River holds the distinction of being the longest river in the world, with a total length of around 6,825 kilometers. The area of 3,349,000 km2 is approximately 10% of Africa's overall landmass. There are many different types of landforms found in the basin, including high mountains, savannas, marshes, tropical forests, woodlands, lakes, arid regions, and deserts. The Nile River Basin traverses 11 countries, namely Burundi, the Democratic Republic of the Congo, Egypt, Eritrea, Ethiopia, Kenya, Rwanda, South Sudan, Sudan, Tanzania, and Uganda [11]. These nations are home to almost 238 million Africans, for whom NRB serves as their primary source of fresh water, energy, and fish. according to [12],the people of these nations will increased to be about 700 million people by 2030.

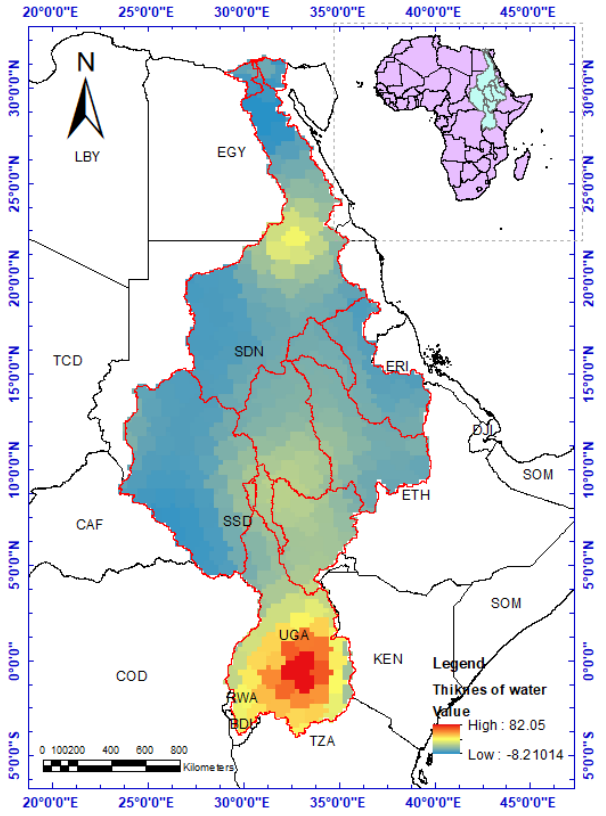

Fig. 1. The Nile River Basin.

The basin's rainfall is exceedingly irregular. The basin has one wet season, usually summer. Only the equator has two rainy seasons. Egyptian and Sudanese desert regions receive little annual rainfall. The basin's vegetation and surface water bodies show rainfall's spatial fluctuation. Runoff is scarce in the Nile watershed. The Ethiopian Highlands, Equatorial Lakes Plateau, and western South Sudan produce the most runoff. The Nile's 3.9% runoff coefficient is due to its tiny runoff-producing area. Total Nile discharge is less than 30 mm across the watershed [13].

2.2. Methodology

The proposed methodology is composed of several key steps as shown in Fig. 2:

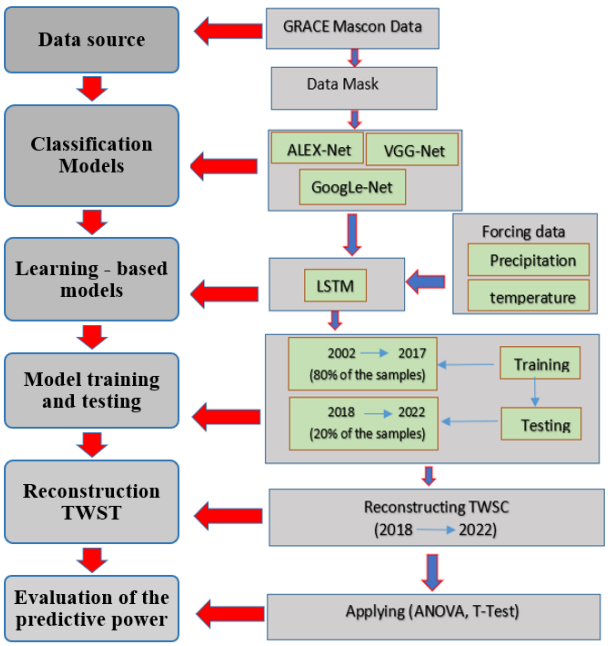

Fig. 2. Flow Chart of Reconstructing of GRAE TWSC for NRB.

2.3. Data used

On a worldwide scale, the hydrological water cycle relies on (TWS) [4]. The total water supply (TWS) is the sum of all the water in the Earth, both above and below ground. This includes both surface water, such as rivers and lakes, and groundwater, as well as any moisture in the soil.in this research, TWSC for the Nile River basin can be determined depending on remote sensing data using GRACE data and applying a deep learning model (LSTM).

GRACE and GRACE-F0 (CSR vO2/ RLO6) mascons with monthly spatial resolution ($1^o \times 1^o$) data that was used in this study are available at this link (http://www2.csr.utexas.edu/grace/RLo6 mascons. html). The Time series data for NRB 2002 to 2022 with about 206 GRACE and GRACE-F0 data are available in NetCDF format, which can be converted to several different forms using a range of tools like ArcMap.TWSC for the Nile River basin from 2002 to 2022, which can be downloaded from the following links(http://gravis.gfz-potsdam.de/land) and (https://grace.jpl.nasa.gov/data-analysis-tool) [14].

GRACE/GRACE-FO data (about 206 months) for NRB was split up into training, and testing sets so that the proposed models could be developed and evaluated. Eighty percent of the available data (165 months, April 2002–July 2018) was utilized for training the model, while the remaining 41 months, July 2018–July 2022, were used for testing the model.

The study of variations in TWS in the Nile River basin relies heavily on precipitation and temperature data. these data are available at(https://p0wer.larc.nasa.g0v/data-access-viewer/).

According to the Climatic Research Unit (CRU), Global Temperature effect on TWSC. The temperature increased and this increased effect on the change of the climate.

2.4. Used Models

The recommended method combines the most beneficial aspects of two different optimization techniques the dipper-throated optimization (DTO) and the fitness grey wolf optimization (GWO) to select the optimal hyperparameters for the LSTM. In this section, we present and investigate the suggested methodology and explain its principles by demonstrating how it might work.

- Extracting features from the image by using multiple CNN models, including Three different networks: AlexNet, VGG Net, and Google Net. (Each of the three models used a different percentage of the data: 80% for training and 20% for validation.).
- Obtaining the most optimal values for the LSTM hyperparameters using an optimization technique (DTOFGW).
- Analyzing and contrasting various optimization algorithms to demonstrate that our proposed model is superior.
- Using statistical analysis tests, such as ANOVA and T-test, to demonstrate the relevance of our suggested model.

2.4.1. Dipper Throated Optimization (DTO)

The concept of "dipper-throated optimization" or "DTO" for short was derived from a model of the basic strategy for foraging which involved monitoring the whereabouts and velocities of aquatic and aerial birds. In order to monitor the birds' swimming paths and speeds, the following mathematical equations are utilized [15].

$$\begin{aligned} BL_{st.nd}\,(t+1) &= BL_{BEST}(t) \\ &- C_1 \cdot |C_2 \cdot BL_{BEST}(t) - BL_{st.nd}\,(t)| \end{aligned} \tag{1}$$

In contrast, the following equation is used to update the flying bird's location. Iteration number t, bird standard locations $BL_{st.nd}\,(t)$ and best location $BL_{BEST}(t)$, and adaptive values C_1 and C_2 are used to adjust the values of these

variables during optimization according to the iteration number and random values.

$$BL_{st.nd}\,(t+1) = BL_{st.nd}\,(t) + BS(t+1) \tag{2}$$

$$\begin{aligned} BS(t+1) = {} & C_3 BS(t) + C_4 r_1\,(BL_{BEST}(t) - BL_{st.nd}\,(t)) \\ & + C_5 r_1\,(BL_{G.BEST} - BL_{st.nd}(t)) \end{aligned} \tag{3}$$

Assuming that C_3 is a weight value, C_4 and C_5 are constants, $BL_{G.BEST}$ is the global best location, r_1 is a random number between 0 and 1 and $BS(t+1)$ is the updated speed of each bird.

2.4.2. Grey Wolf Optimization (GWO)

Grey wolves are considered a top-tier predator on our planet that can be discovered in many different regions. The grey wolf typically inhabits packs. The typical group size is between five and twelve people. The fascinating social hierarchy of grey wolves is a crucial feature of this species. Both male and female alphas are dominant in packs. The alpha makes major group decisions like where to go hunts, whether to take breaks, etc. Everyone in the group must listen to and obey the alpha's orders. The alpha wolf has been observed to follow the pack's lead, which some have interpreted to mean that wolves practice democracy [16].

There are two distinct social classes among grey wolves, with Beta occupying the bottom. The beta wolf is a subordinate member of the pack who supports the alpha wolf by providing information and advice. While the alpha is the pack's top dog, the betas are responsible for the rest of the pack members. A wise advisor to the alpha and a firm upholder of group norms, they serve dual roles. Alphas rely on their subordinates, the betas to carry out their orders and get feedback from the group on how things are progressing. Omega is the lowest-ranking member of the grey wolf pack. Omega steps in as the scapegoat. Despite their best efforts, omega wolves are always pushed around by the pack's alphas. As the last of the wolf population, they are also allowed to eat meat. Even if the omegas aren't highly regarded, losing even one of them could cause friction and problems for the rest of the group. The omegas express the emotions shared by the entire pack of wolves. Since everyone has needs that must be met, omegas are essential in maintaining equilibrium. If a wolf doesn't make alpha, Beta, or Omega, it's automatically looked down upon. Delta wolves oversee the Omega, and all the other packs must answer them. People of all ages and roles, from scouts to seniors to hunters, make up this group. Since the hunters help the alphas and betas bring down prey, everyone in the pack benefits from their efforts. The sentinels' job is to keep everyone safe and defend the group from threats. The primary role of a scout is to patrol and report on the territory of the group, looking for potential dangers and reporting them to the rest of the group. Wolves who have held the positions of alpha or beta within the pack are regarded as elders. While the social structure of the grey wolf pack is fascinating, the cooperative hunting strategy employed by the group is perhaps more fascinating. Grey wolves, as we said before, are currently surrounding their prey. For mathematical modeling of encircling behavior, the following equations are proposed.

$$\overrightarrow{D} = \left| \overrightarrow{C} \cdot \overrightarrow{F}_p(t) - \overrightarrow{F}\,(t) \right| \tag{4}$$

$$\vec{F}(t+1) = \vec{F}_p(t) - \vec{A} \cdot \vec{D} \tag{5}$$

Assume $\vec{A}$ and $\vec{C}$ be coefficient vectors, t be the current iteration, $\vec{F}$ be the position vector of the grey wolf, and $\vec{F}_p$ be the position vector of the prey. Once a superior solution is found on each iteration, the vector F is changed to reflect this optimal solution.

$$\vec{a} = 2 - t\left(\frac{2}{\text{Max}_{\text{iter}}}\right) \tag{6}$$

$$\overrightarrow{A} = 2\overrightarrow{a} \cdot \overrightarrow{r}_1 - \overrightarrow{a} \tag{7}$$

$$\overrightarrow{C} = 2\overrightarrow{r}_2 \tag{8}$$

A random vector $\vec{r}_1$ and $\vec{r}_2$ in the interval $[0,1]$ and $\vec{a}$ that falls linearly from 2 to 0 as the number of iterations increases are represented by the variables Max_{iter} and the loop counter t . To begin investigating the effects of Eqs. (1) and (2), think about a two-dimensional position vector and a few of the possible neighbors. A gray wolf in this scene can change its location from (X, Y) to (X^*, Y^*) to follow the movement of its prey. By adjusting the current values of the EA and EC vectors, one can go to other regions surrounding the ideal agent. For instance, if you set $\vec{A} = (1,0)$ and $\overrightarrow{C} = (1,1)$, you'll get $(X^* - X, Y^*)$. The grey wolf can use the random vectors r 1 and r 2 to go from one location to another. Using Eqs. (1) and (2), a grey wolf can alter its stance when it is close to its victim. Using the same strategy in different dimensions, the grey wolves will circle the optimal solution up to this point, which may be a hypersphere or a cube.

It is possible for a grey wolf to locate its victim and then surrounding it. Typically, the alpha is the one in charge when hunting. On rare occasions, the search will be joined by both the Beta and the delta. But in our simulated 2D search area, we still don't know where the prey could be hiding (ideal). For the sake of building a statistical model of the grey wolf pack's foraging behaviors, we will assume that the alpha, beta, and delta wolves all have a common knowledge of the territory's finest hunting sites. Hence,

we will save the first three results and make the other grey wolves (including the omegas) use them to re-ascertain their positions. Therefore, we came up with these equations:

$$\vec{D}_\alpha = \left|\vec{D}_1 * \vec{F}_\alpha - \vec{F}\right|, \quad \vec{D}_\beta = \left|\vec{D}_2 * \vec{F}_\beta - \vec{F}\right|, \quad \vec{D}_\delta = \left|\vec{D}_3 * \vec{F}_\delta - \vec{F}\right| \tag{9}$$

$$\vec{F}_1 = \vec{F}_\alpha - \vec{A}_1 * \vec{D}_\alpha, \quad \vec{F}_2 = \vec{F}_\beta - \vec{A}_2 * \vec{D}_\beta \quad \vec{F}_3 = \vec{F}_\delta - \vec{A}_3 * \vec{D}_\delta \tag{10}$$

$$\vec{F}(t+1) = \frac{\vec{F}_1 + \vec{F}_2 + \vec{F}_3}{3} \tag{11}$$

Features Extraction Models An existing model has previously been developed and evaluated on a large dataset to tackle a similar challenge. Machine Learning teams can employ pre-trained models as a foundation for their work, rather than beginning from the ground up. Large-scale effectiveness has been demonstrated by pre-trained language models like the Generative Pre-trained Transformer (GPT-n) series and Bidirectional Encoder Representations from Transformers (BERT) [17]. pre-trained models are used for a quick start in text and image processing [18].

The classification technique in this research utilized models that had been trained such as AlexNet, VGG Net, and Google Net., and the best model was used to extract features. After that, LSTM models were used for the classification process, using an optimization algorithm (DTOFGW) to get the best hyperparameters for LSTM. Finally, comparing many different optimization algorithms shows our proposed model's superiority.

2.4.3. Configurations parameters for the proposed model

Optimal LSTM hyperparameters were obtained using a model that combines two optimization techniques: fitness grey wolf optimization (GWO) and dip-throated optimization (DTO). The name of the suggested model is (DTOFGW-LSTM. The proposed DTOFGW was applied to obtain the best LSTM hyperparameters as shown in Table 1.

2.4.4. Model Evaluation Criteria

The LSTM-DTOFGW model was evaluated using the ANOVA test, Accuracy, Sensitivity (TPR), Specificity (TNR), P value (PPV), N value (NPV), and F-score. The real positive rate (TPR) of a test is the percentage of diseased persons who will test positive. True Negative Rate (TNR) is the percentage of healthy patients who get a negative test result; F-score is a harmonic average of precision and recall; P-value is probability value. The P-value indicates the likelihood of a result that is similar or slightly more intense than the others. A higher accuracy means the model's predictions match the ground truth's labels or values. Sensitivity (true positive rate) is the likelihood of a positive test result if the person is positive; Specificity (true negative rate) is the probability of a negative test result if the person is negative [19]. These variables are calculated as following:

- Accuracy $= \frac{\text{T.P+T.N}}{\text{T.P+FP+T.N+F.N}}$
- Sensitivity $= \frac{\text{T.P}}{\text{T.P} + \mathbf{F \cdot N}}$
- Specificity $= \frac{\text{T.N}}{\text{T.N} + \text{F.P}}$
- F -score $= \frac{2\text{TP}}{2T.P+F \cdot P+F \cdot N}$
- P-value $= \frac{P-P0}{\sqrt{\frac{P(1-P0)}{n}}}$

Where:

T.P: True Positive
T.N: True
F.P: False Positive
F.N: False Negative
P: Sample Proportion
P0 : Hypothesized Proportion
n: Sample Size

3. Results

3.1. Reconstructing TWSC for NRB

Fig. 3a shows the difference between TWSC(CSR) and the TWSC(DTOFGW-LSTM) for 41 samples of time series data.

The proposed model was used to identify terrestrial water storage data during the GAP period of GRACE from 2017 to 2018($\sim$1 year) and the data of terrestrial water storage changes ranged from -0.17927mm to 14.03725mm as shown in Fig. 3b.

3.2. Performance Metrics for Models of Classification

First Stage: The first experiment is designed to investigate the classification accuracy of three CNN models (VGG-Net, Alex Net Google Net) as shown in Table 2. These models are used for features extraction.80% of GRACE data are used for the classification process and the remaining data were used for the validation process, the results of the classification process appeared the outperformance of Google Net model over the other two models for the process of features extraction by 87.8%accuracy.

Second Stage: Four optimisation algorithms were used to optimise the parameters of an LSTM deep network, demonstrating the superiority of the proposed approach(DTOFGW).these models are: Particle Swarm Optimization (PSO), Grey Wolf Optimizer (GWO), Whale Optimization Algorithm (WOA) and Dipper Throated Optimization (DTO). The proposed DTOFGW compared to

Table 1. The Proposed DTOFGW Algorithm.

The suggested DTOFGW method	
	Get started Birds Locations $(BL)_i (i = 1, 2, 3, 4, \ldots\ldots, n)$ with size n, $BS_i (i = 1, 2, 3, \ldots, n)$, Fitness assessment Fn, $f_2, r_1, r_2, r_3, R, C_1, C_2, C_3, C_4, C_5, t = 1$, and max iterations max_{iter}
	Evaluate Fitness assessment Fn for each $(BL)_i$
1	**Find** best bird BL_{BEST}
2	**While** $t < iter \quad max$ **do**
3	**for** $(i = 1; i \leq n)$ **do**
4	**If** $(Z < 0.5)$ **then**
5	**Update** The gey wolf operatives' position as determined by:
6	**Update** (fitness)Strength training $\overrightarrow{F\alpha} = \left(\vec{F}_\alpha / \left(\vec{F}_\alpha + \vec{F}_\beta + \vec{F}_\delta\right)\right.$
7	**Update** (fitness) Strength training $\vec{F}_\beta = \left(\vec{F}_\alpha / \left(\vec{F}_\alpha + \vec{F}_\beta + \vec{F}_\delta\right)\right.$
8	**Update** (fitness)Strength training $\vec{F}_\delta = \left(\vec{F}_\alpha / \left(\vec{F}_\alpha + \vec{F}_\beta + \vec{F}_\delta\right)\right.$
9	$\vec{D}_\alpha = \left\lvert \vec{D}_1 * \vec{F}_\alpha - \vec{F} \right\rvert, \vec{D}_\beta = \left\lvert \vec{D}_2 * \vec{F}_\beta - \vec{F} \right\rvert, \vec{D}_\delta = \left\lvert \vec{D}_3 * \vec{F}_\delta - \vec{F} \right\rvert$
10	**else**
11	**Update** Speed of the flying bird using:
12	$BS(t+1) = C_3 BS(t) + C_4 r_1 \left(BL_{BEST}(t) - BL_{st.nd}(t)\right)$
13	$+C_5 r_1 \left(BL_{G.BEST} - BL_{st.nd}(t)\right)$
14	**Update** The swimming bird's position as determined by:
15	$BL_{\text{st.nd}}(t+1) = r_1 + z * r_2 + (1 - z) * r_3 + BS(t+1)$
16	**end after**
17	**end after**
18	**Evaluate** Fitness assessment F n for each $\overrightarrow{BL_l}$
19	**Update** $R, r_1, r_2, r_3, c, C_1, C_2$
20	**Find** best bird BL_{best}
21	**Set** $BL_{G.BEST} = BL_{BEST}$
22	**Set** $t = t + 1$
23	**end when**
24	**return** $BL_{G.BEST}$

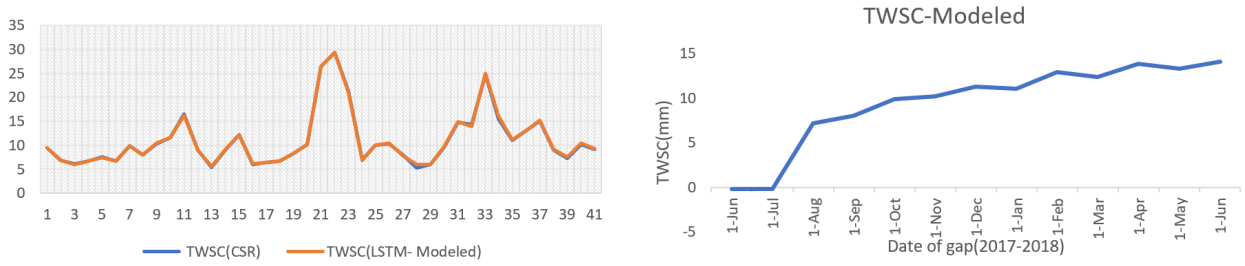

Fig. 3. (a) Difference between GRACE Data and TWSC for the Proposed Model, (b) Data of TWSC during gap period (2017-2018).

these models and the performance matrices as shown in Table 3. In this table, the proposed model shows the best performance among the other models.

The results of statistical analysis and One Sample T-Test are presented in Table 4. This analysis is performed to show the proposed approach's stability compared to the other models. The p-value in these tables is less than 0.05, proving the statistical difference between the proposed model and the other models [20, 21]. the proposed model outperformed the other models.

Fig. 4 represents the visual plots for the results of the ANOVA- Test. This figure is composed of four plots: residual, homoscedasticity, quartile–quartile QQ, and heatmap plot. The results of the plots prove the proposed method's effectiveness and superiority over the other models. Fig. 5 illustrates the accuracy of LSTM models, and the histogram displays the resulting accuracy for these models. The chart shows that DTOFGW-LSTM outperformed the other models with 96.8

Table 2. Performance Matrices for CNN Models used for extracting features.

Models	Accuracy	Sensitivity (TPR)	Specificity (TNR)	P value (PPV)	N value (NPV)	F-score
VGG-Net	0.829268293	0.444444444	0.9375	0.666667	0.857143	0.533333333
Alex Net	0.846320346	0.445652174	0.945945946	0.672131	0.872818	0.535947712
Google Net	0.878444084	0.432989691	0.961538462	0.677419	0.900901	0.528301887

Table 3. Performance Matrices for The Proposed Model and Other Models.

Models	Accuracy	Sensitivity (TPR)	Specificity (TNR)	P value (PPV)	N value (NPV)	F-score
LSTM	0.900643317	0.344827586	0.979591837	0.705882353	0.913242	0.4633205
WOA-LSTM	0.919811321	0.344827586	0.985545335	0.731707317	0.929368	0.46875
PSO-LSTM	0.921198668	0.333333333	0.986436498	0.731707317	0.930233	0.4580153
GWO-LSTM	0.92745377	0.27184466	0.998423542	0.949152542	0.926829	0.4226415
DTO-LSTM	0.935956467	0.27184466	0.998625744	0.949152542	0.935622	0.4226415
DTOFGW-LSTM	0.967868339	0.5	0.995024876	0.853658537	0.97166	0.6306306

Table 4. Statical Analysis and One Sample T-Test.

Descriptive Statistics	LSTM	WOA-LSTM	PSO-LSTM	GWO-LSTM	DTO-LSTM	DTOFGW-LSTM
Number of values	10	10	10	10	10	10
Minimum	0.8991	0.9098	0.9112	0.9175	0.926	0.9678
25%Percentile	0.9006	0.9198	0.9212	0.9275	0.936	0.9679
Median	0.9006	0.9198	0.9212	0.9275	0.936	0.9679
75% Percentile	0.9006	0.9198	0.9212	0.9275	0.936	0.9679
Maximum	0.9096	0.921	0.9261	0.9375	0.946	0.9679
Range	0.01058	0.01117	0.01492	0.02	0.02	0.00013
Mean	0.9014	0.9189	0.9207	0.9275	0.936	0.9679
Std. Deviation	0.002944	0.003224	0.003676	0.004714	0.004714	0.00003401
Theoretical mean	0	0	0	0	0	0
Actual mean	0.9014	0.9189	0.9207	0.9275	0.936	0.9679
One sample, t test t df	t=968.3, df=9	t=901.2, df=9	t=792.0, df=9	t=622.2, df=9	t=627.9, df=9	t=89993, df=9
Range	0.01058	0.01117	0.01492	0.02	0.02	0.00013
Mean	0.9014	0.9189	0.9207	0.9275	0.936	0.9679
hline Std. Deviation	0.002944	0.003224	0.003676	0.004714	0.004714	0.00003401
Theoretical mean	0	0	0	0	0	0
Actual mean	0.9014	0.9189	0.9207	0.9275	0.936	0.9679
Number of values	10	10	10	10	10	10
P value (two tailed)	< 0.0001	< 0.0001	< 0.0001	< 0.0001	< 0.0001	< 0.0001
P value summary	****	****	****	****	****	****
Significant (alpha=0.05)?	Yes	Yes	Yes	Yes	Yes	Yes
How big is the discrepancy?						
Discrepancy	0.9014	0.9189	0.9207	0.9275	0.936	0.9679
SD of discrepancy	0.002944	0.003224	0.003676	0.004714	0.004714	0.00003401
SEM of discrepancy	0.0009309	0.00102	0.001163	0.001491	0.001491	0.00001075
95% confidence interval	0.8993 to 0.9035	0.9166 to 0.9212	0.9181 to 0.9233	0.9241 to 0.9308	0.9326 to 0.9393	0.9678 to 0.9679
R squared (partial eta	1	1	1	1	1	1

4. Discussion

Deep learning models (Alex Net, VGG-Net, and Google Net) that were used in this research to classify GRACE and GRACE-FO data over Nile River Basin showed satisfying results. Google Net model has outperformed the other two models with 87.8%accuracy, 0.433 Sensitivity, 0.962 Specificity, 0.677 P value, 0.901 N value and 0.528 F-score. So, this model was used to extract features from GRACE GeoTiff data to use this data after that in the reconstructing process of TWS data over NRB. in this research, (165 monthly GRACE data) were used as training data for the period from 2002 to 2018 and (41 monthly GRACE-FO

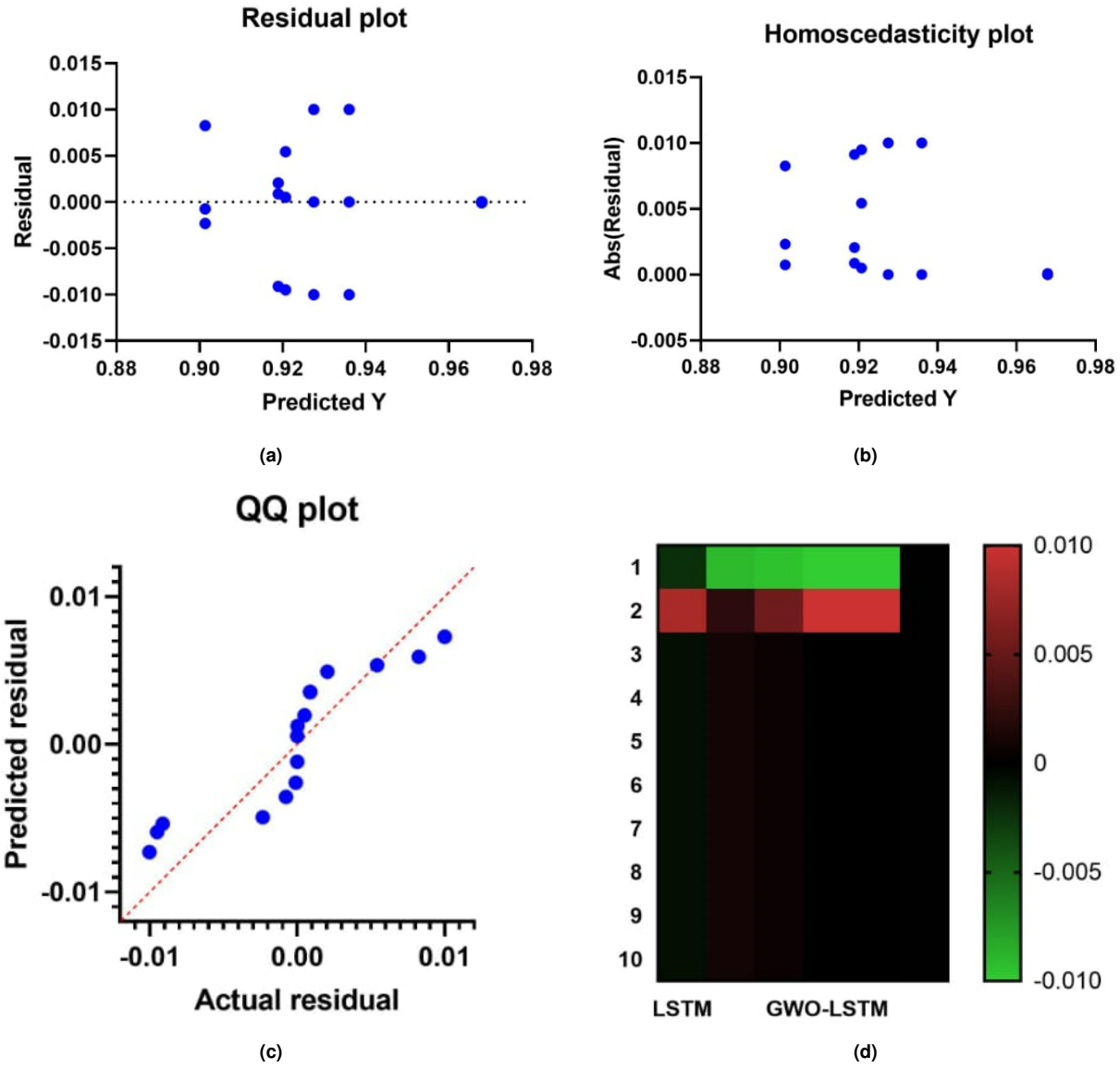

Fig. 4. Results of ANOVA- Test as,(a) represents Residual plot,(b)represents homoscedasticity plot,(c)represents QQ plot,(d) heatmap plot.

data) were used to validate data for the period from 2018 to 2022 with taking into consideration the meteorological data (precipitation and temperature) as a parameter affecting on the classification and the reconstructing process. The proposed model (DTOFGW-LSTM) showed the best results for the reconstructing process compared with the other models (LSTM, WOA-LSTM, PSO-LSTM, GWO-LSTM, and DTO-LSTM). DTOFGW-LSTM outperformed better than different models by 96.8%accuracy, 0.5 Sensitivity, 0.995 Specificity, 0.854 P value, 0.972 N value, and 0.631 F-score. Fig. 5 shows the accuracy for the different models, and the histogram of the accuracy. ANOVA test for the proposed model has been conducting a satisfying result with P Value (P<0.0001) and the results of one sample T-Test, SD of discrepancy (0.00003401), (R^2 = 1) and 95% confidence interval (0.9678 to 0.9679). Fig. 4 shows the results of the ANOVA test for the proposed model. The proposed model had a superior performance in the statical analysis compared to the other models with Mean 0.9679, Std. Deviation 0.00003401 and Std. The error of Mean 0.00001075. The reconstructing of data for the period 2002 to 2022 over NRB showed the similarity of the values of TWSC from the proposed model with the values of TWSC from GRACE data. The values of the TWSC for NRB from the proposed model showed

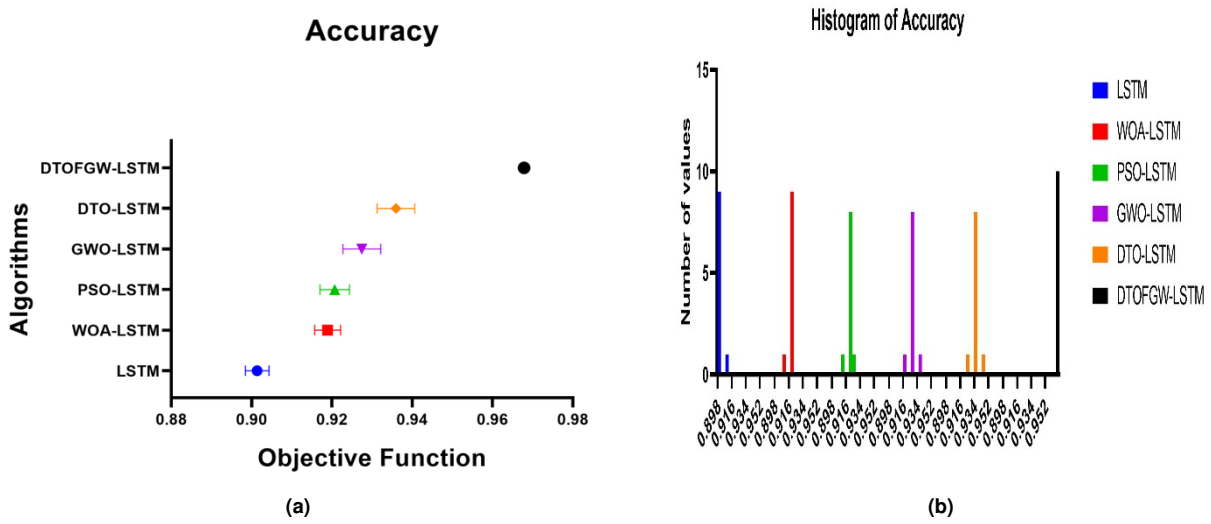

Fig. 5. (a)Value of Accuracy for LSTM models, and(b) Histogram of Accuracy for LSTM models.

an increase in the values of TWSC, the highest and lowest reconstructing water change over NRB between the period from 2018 to 2022 equal 29.36 mm in July 2020 and 5.56 mm in October 2019 respectively. The results of TWSC that have been obtained from the proposed model(LSTM-DTOFGW) showed the extent of convergence and conformity between it and the actual values of GRACE data and its superiority over the model used by [22] in evaluating TWSC in NRB.

5. Conclusion

The primary objective of this research was to reconstruct GRACE and GRACE-FO data over (NRB)using a significant amount of time series data for the period from 2002 to 2022, and studying the occurrence of drought or not in the study area during the GAP period, based on the analysis of data in the years before and after the GAP period, taking into account weather data of temperatures and precipitation in the study area during the GAP period. Three deep learning (DL) models (Alex Net, VGG-Net, and Google Net) were applied for the classification and the process of extracting features, the model with high accuracy was used to extract features from the time series data. Google Net outperformed the other two models in extracting the variables that most influence the process of reconstructing GRACE data. Then it can be concluded that:

1. The proposed model (DTOFGW-LSTM) outperformed the other models (LSTM, WOA-LSTM, PSO-LSTM, GWO-LSTM, and DTO-LSTM) with 96.8%accuracy.
2. The ANOVA and t-test were used to analyze the resulting data. It has been shown that the TWS estimates of NRB are consistently positive (>0 cm) over all years under consideration.
3. The proposed model was based on the weather variables that have the most influence on the terrestrial water storage in the Nile River Basin, which are temperatures and precipitation as basic variables in building the proposed model.
4. The results of the proposed model used to reconstruct the data of the terrestrial water storage in the NRB showed a change by an amount ranges between (5.56 to 29.36mm) during the validation period(2018 to 2022) and These results were compared to the values of the change in the terrestrial water storage obtained from GRACE data, and it was proven that the data simulated accurately matched with a maximum precision of 96.3%.
5. Then, the proposed model was used to identify terrestrial water storage data during the GAP period of GRACE from 2017 to 2018(sim1 year) and the amount of terrestrial water storage changes ranged from-0.17927mm to 14.03725mm.

Finally, the proposed model (DTOFGW-LSTM) is the best model for reconstructing GRACE data for NRB and could be applied to predict TWSC for the following years. Thus, it can be known whether future problems will occur due to an increase or decrease in the amount of water in the NRB. the proposed model could be used to predict TWSC and GWSC using time series data from other satellite like SWARM, taking into consideration more data about the

climate change and Applying new A.I models for classification process.

References

[1] M. H. M. M. Elsanabary, (2012) *"Teleconnection, Modeling, Climate Anomalies Impact and Forecasting of Rainfall and Streamflow of the Upper Blue Nile River Basin"* **Unknown Journal *Unknown Volume***: Unknown Pages. DOI: UnknownDOI.

[2] J. Sheffield, E. F. Wood, M. Pan, H. Beck, G. Coccia, and A. Serrat-Capdevila, (2018) *"Satellite Remote Sensing for Water Resources Management: Potential for Supporting Sustainable Development in Data-Poor Regions"* **Water Resources Research *54***: 9724–9758. DOI: 10.1029/2017WR022437.

[3] T. Oki and S. Kanae, (2006) *"Global Hydrological Cycles and World Water Resources"* **Science *313***: 1068–1072. DOI: UnknownDOI.

[4] N. Tangdamrongsub, M. F. Jasinski, and P. J. Shellito, (2021) *"Development and Evaluation of 0.05g Terrestrial Water Storage Estimates Using Community Atmosphere Biosphere Land Exchange (CABLE) Land Surface Model and Assimilation of GRACE Data"* **Hydrology and Earth System Sciences *25***: 4185–4208. DOI: 10.5194/hess-25-4185-2021.

[5] Z. Sun and D. Long, (2020) *"Reconstruction of GRACE Data on Changes in Total Water Storage Over the Global Land Surface and 60 Basins"* **Water Resources Research**: 1–21. DOI: 10.1029/2019WR026250.

[6] F. W. Landerer and S. C. Swenson, (2012) *"Accuracy of Scaled GRACE Terrestrial Water Storage Estimates"* **Water Resources Research *48***: 1–11. DOI: 10.1029/2011WR011453.

[7] G. O. Ahi and H. O. Cekim, (2021) *"Long-Term Temporal Prediction of Terrestrial Water Storage Changes Over Global Basins Using GRACE and Limited GRACE-FO Data"* **Acta Geodaetica et Geophysica *56***: 321–344. DOI: 10.1007/s40328-021-00338-4.

[8] G. O. Ahi and S. Jin, (2019) *"Hydrologic Mass Changes and Their Implications in Mediterranean-Climate Turkey from GRACE Measurements"* **Remote Sensing *11***: 1–24. DOI: 10.3390/rs11020120.

[9] Z. M. Nigatu, D. Fan, and W. You, (2021) *"GRACE Products and Land Surface Models for Estimating the Changes in Key Water Storage Components in the Nile River Basin"* **Advances in Space Research *67***: 1896–1913. DOI: 10.1016/j.asr.2020.12.042.

[10] S. Mo, Y. Zhong, E. Forootan, N. Mehrnegar, X. Yin, and J. Wu, (2022) *"Bayesian Convolutional Neural Networks for Predicting the Terrestrial Water Storage Anomalies During GRACE and GRACE-FO Gap"* **Journal of Hydrology *604***: 1–27. DOI: 10.1016/j.jhydrol.2021.127244.

[11] E. Hasan and A. Tarhule, (2019) *"Trend Dynamics of GRACE Terrestrial Water Storage in the Nile River Basin"* **Preprints**: 14–23. DOI: 10.20944/preprints201909.0042.v1.

[12] M. El-Fadel, Y. El-Sayegh, K. El-Fadl, and D. Khorbotly, (2003) *"The Nile River Basin: A Case Study in Surface Water Conflict Resolution"* **Journal of Natural Resources and Life Sciences Education *32***: 107–117. DOI: UnknownDOI.

[13] T. N. B. Initiative. *The Water Resources of the Nile Basin*. State River Nile Basin, 2012, 25–56.

[14] Y. Shen, W. Zheng, W. Yin, A. Xu, H. Zhu, and Q. Wang, (2022) *"Improving the Inversion Accuracy of Terrestrial Water Storage Anomaly by Combining GNSS and LSTM Algorithm and Its Application in Mainland China"* **Remote Sensing *14***: DOI: 10.3390/rs14030535.

[15] A. E. Takieldeen, E.-S. M. El-kenawy, M. Hadwan, and R. M. Zaki, (2022) *"Dipper Throated Optimization Algorithm for Unconstrained Function and Feature Selection"* **Computational Materials Continuum *72***: 1465–1481. DOI: UnknownDOI.

[16] S. Mirjalili, I. Aljarah, M. Mafarja, A. A. Heidari, and H. Faris, (2020) *"Grey wolf optimizer: theory, literature review, and application in computational fluid dynamics problems"* **Nature-inspired optimizers: Theories, literature reviews and applications**: 87–105.

[17] X. Han, Z. Zhang, N. Ding, Y. Gu, X. Liu, and Y. Huo, (2021) *"Pre-Trained Models: Past, Present and Future"* **Unknown Journal**: DOI: UnknownDOI.

[18] X. Qi, T. Sun, Y. Xu, Y. Sun, N. Dai, and X. Huang, (2020) *"Pre-Trained Models for Natural Language Processing: A Survey"* **Unknown Journal**: DOI: UnknownDOI.

[19] A. G. Glaros and R. B. Kline, (1988) *"Understanding the Accuracy of Tests with Cutting Scores: The Sensitivity, Specificity, and Predictive Value Model"* **Journal of Clinical Psychology *44***: 1013–1023. DOI: UnknownDOI.

[20] M. M. Eid, E.-S. M. El-Kenawy, N. Khodadadi, S. Mirjalili, E. Khodadadi, M. Abotaleb, A. H. Alharbi, A. A. Abdelhamid, A. Ibrahim, G. M. Amer, et al., (2022) *"Meta-heuristic optimization of LSTM-based deep network for boosting the prediction of monkeypox cases"* **Mathematics *10***(20): 3845.

[21] E.-S. M. El-Kenawy, S. Mirjalili, A. A. Abdelhamid, A. Ibrahim, N. Khodadadi, and M. M. Eid, (2022) *"Meta-heuristic optimization and keystroke dynamics for authentication of smartphone users"* **Mathematics *10***(16): 2912.

[22] M. Abd-Elbaky and S. Jin, (2019) *"Hydrological Mass Variations in the Nile River Basin from GRACE and Hydrological Models"* **Geodesy and Geodynamics *10***: 430–438. DOI: 10.1016/j.geog.2019.07.004.